Received: 16 April 2020 | Revised: 12 August 2020 | Accepted: 21 August 2020

DOI: 10.1096/fj.202000912RR

RESEARCH ARTICLE

THE FASEB JOURNAL

Characterization of the complex of the lysosomal membrane transporter MFSD1 and its accessory subunit GLMP

David Massa López[1] | **Lea Kählau**[1] | **Katharina Esther Julia Jungnickel**[2] | **Christian Löw**[2] | **Markus Damme**[1]

[1]Institute of Biochemistry, Christian-Albrechts-University Kiel, Kiel, Germany

[2]Centre for Structural Systems Biology (CSSB), DESY and European Molecular Biology Laboratory Hamburg, Hamburg, Germany

Correspondence
Markus Damme, Institute of Biochemistry, Christian-Albrechts-University Kiel, Olshausenstr. 40, 24098 Kiel Germany.
Email: mdamme@biochem.uni-kiel.de

Funding information
This work was in part supported by the Deutsche Forschungsgemeinschaft (DFG) to MD (DA 1785-1).

Abstract

The two lysosomal integral membrane proteins MFSD1 and GLMP form a tight complex that confers protection of both interaction partners against lysosomal proteolysis. We here refined the molecular interaction of the two proteins and found that the luminal domain of GLMP alone, but not its transmembrane domain or its short cytosolic tail, conveys protection and mediates the interaction with MFSD1. Our data support the finding that the interaction is essential for the stabilization of the complex. These results are complemented by the observation that N-glycosylation of GLMP in general, but not the type of N-glycans (high-mannose-type or complex-type) or individual N-glycan chains, are essential for protection. We observed that the interaction of both proteins already starts in the endoplasmic reticulum, and quantitatively depends on each other. Both proteins can affect vice versa their intracellular trafficking to lysosomes in addition to the protection from proteolysis. Finally, we provide evidence that MFSD1 can form homodimers both in vitro and in vivo. Our data refine the complex interplay between an intimate couple of a lysosomal transporter and its accessory subunit.

KEYWORDS

accessory subunit, GLMP, lysosomal, MFSD1, transporter

1 | INTRODUCTION

The major function of lysosomes is the hydrolytic breakdown of various macromolecules including proteins, lipids, nucleic acids, and oligosaccharides, to low-molecular-weight metabolites which can be re-used in the cytosol for biosynthetic pathways.[1] The resulting low-molecular-weight degradation products are exported via the limiting lysosomal membrane to the cytosol by the action of numerous transporter proteins, of which many are still enigmatic.[2] Some transporter proteins actively import a subset of metabolites from the cytosol into the lysosomal lumen.[3]

The great majority of lysosomal proteins including integral transmembrane proteins are highly N-glycosylated, a posttranslational modification that has evolved for protecting the lumen-exposed loops from the harsh conditions of the lysosomal matrix, which exhibits an acidic pH, a high concentration of active proteases, and reducing conditions.[4,5] Some polytopic integral membrane proteins lack N-glycosylation, but tightly interact with accessory subunits, which take over

Abbreviations: EndoH, endoglycosidase H; ER, endoplasmic reticulum; FRET, fluorescence resonance energy transfer; HA, human influenza hemagglutinin; MEF, mouse embryonic fibroblasts; PNGaseF, peptide-N-glycosidase F; TMD, transmembrane domain.

the protective function.[6-9] In addition to their protective role, such accessory subunits furthermore often affect intracellular sorting of the protein complexes and even affect transport activity in the case of transporters.[7,8,10,11]

Recently, we have characterized a novel lysosomal multiple transmembrane-spanning protein, MFSD1, that was initially identified by proteomic analysis of enriched lysosomes and is supposed to transport small solutes across the lysosomal membrane.[2,9] MFSD1 has 12 transmembrane helices and belongs to the major facilitator superfamily (MFS), one of the two largest families of transporter proteins that mediate secondary active or passive transport in different cellular compartments.[12] MFSD1 is not N-glycosylated and localizes in lysosomes of mouse embryonic fibroblasts (MEF) and other cell types in various mouse tissues.[9] MFSD1 is critical for liver homeostasis and MFSD1-deficiency in mice leads to a liver disease characterized by the partial loss of sinusoids, the extravasation of erythrocytes, development of liver fibrosis, and sporadic tumor development at a late stage of age. We found that MFSD1 critically depends on the highly N-glycosylated lysosomal type I transmembrane protein GLMP and *vice versa*: MFSD1 and GLMP stability depends on each other, in a way that the absence of MFSD1 leads to an almost complete decline of GLMP protein levels, and the absence of GLMP leads to similar decline of MFSD1. *Glmp* knockout mice suffer from a liver injury that strikingly resembles the phenotype observed in *Mfsd1* knockout mice,[9,13] supporting the tight genetic interaction between the two proteins.

Here we refined the interaction between MFSD1 and GLMP and found the highly glycosylated luminal domain of GLMP to be essential and sufficient to interact with MFSD1. We, therefore, studied in more detail the N-glycosylation of GLMP and the importance of N-glycosylation for GLMP stability. We found evidence that MFSD1 and GLMP already start to form a complex in the endoplasmic reticulum (ER) and that the interaction of both proteins affects their intracellular sorting. The two complex-partners quantitatively depend on each other and if one subunit is limiting, the consequence is increased proteolytic degradation of the other interaction partner, implicating a balanced and regulated stoichiometry. Finally, we provide evidence that MFSD1 can form homodimers in vitro and in vivo. Our findings provide a more detailed insight into the interdependence of an intimate couple that is essential for stability but also affects intracellular trafficking.

2 | MATERIALS & METHODS

2.1 | Antibodies and reagents

Antibodies against MFSD1 and GLMP were described previously.[9] The following commercial and noncommercial antibodies were used throughout the study: LAMP2 (clone H4B4, Developmental Studies Hybridoma Bank), HA (clone 3F10; Roche), HA-Peroxidase (clone 3F10; Roche), HA (clone F7; Santa Cruz), GAPDH (Santa Cruz), LAMP1 (clone 1D4B, Developmental Studies Hybridoma Bank), Tubulin (Clone E7; Developmental Studies Hybridoma Bank), LAMP2 (clone ABL93; Developmental Studies Hybridoma Bank), GM130 (Clone 35/GM130, BD Bioscience), HA-PE (Clone 16B12; Biolegend), CD63 (Eurogentec), KDEL (clone 10C3; Enzo Life Sciences), PDI (clone 1D3; Enzo Life Sciences), LBPA (clone 6C4, gift from Jean Gruenberg), LIMP2 (Pineda), PLD3,[14] GFP (clones 7.1 and 13.1; Roche), CoxIV (Abcam), and mouse Trueblot ULTRA (Rockland). All standard reagents and chemicals, if not stated otherwise, were purchased from Sigma-Aldrich.

2.2 | Plasmids

mMFSD1, mMFSD8, and hLAMP1 constructs were cloned using murine mMFSD1-influenza hemagglutinin (HA) in the pcDNA3.1 vector, mMFSD8 pEGFP-N1, and hLAMP1-HA pcDNA3.1 as templates, respectively. A sequence coding for the α2c-adrenergic receptor ER-retention motif (KHILFRRRRRGFRQ) was introduced in the cloning primer and fused at the C-terminus of the mMFSD1-HA sequence. The mutations MFSD1^{11,12LL_AA} and GLMP^{400Y_A} were introduced in the cloning primer and by site-directed mutagenesis, respectively. The mutations N_A of GLMP putative N-glycosylation sites were introduced by site-directed mutagenesis. The GLMP-LAMP1 chimeras were generated by PCR-driven overlap extension using mGLMP-HA-pcDNA3.1 and hLAMP1-HA pcDNA3.1 as templates. Primers containing restriction sites XhoI/HindIII (mMFSD1), NotI/NotI (mMFSD1), Xho/BamHI (GLMP and hLAMP1), and BglII/HindIII (mMFSD8) were purchased from Sigma-Aldrich. mMFSD1 was cloned into pEGFP-C1 and pXLG, mMFSD8 was cloned into pmKATE2 and hLAMP1 was cloned into pEGFP-N1 vector. All constructs were sequenced by GATC Biotech (Cologne, Germany).

2.3 | Cell culture and transfection

MEFs from wild type, *Mfsd1* knockout, and *Glmp* knockout mice were described previously.[9] MEFs and HeLa cells were cultivated in DMEM containing 4.5 g/L of D-glucose, L-glutamine (Thermo Fisher Scientific) supplemented with 10% (v/v) fetal bovine serum (FBS; Biochrom), 100 units/ml penicillin (Life-technologies), and 100 µg/mL streptomycin (Life-technologies). MEF *Glmp* KO and MEF wild-type cells were cultured with 1 µg/mL of kifunensine (Cayman) for a period from 48 to 72 hours. After 48 hours of treatment with

kifunensine, MEF *Glmp* KO cells were treated for additional 9 or 24 hours with 20mU/mL of EndoH (Roche) in addition to 1 µg/mL kifunensine.

A mix of 1-5 µg of DNA (depending on the experiment) incubated with polyethylenimine (PEI) in DMEM (without antibiotics and FBS) for 15 minutes at room temperature (RT) was used for transfection of cells. The mix was applied to the culture of cells and after ~6 hours, the cell culture medium was exchanged. The transfected cells were analyzed, if not indicated otherwise, 24-48 hours post-transfection.

2.4 | Purification of mMFSD1

HEK293F cells at a cell density of 20×10^6 cells/ml were transiently transfected with mMFSD1-GFP-His pXLG plasmid using PEI. After incubation for 3 hours at 8% CO_2, 37°C, FreeStyle 293 Expression Medium was added to reach a final cell density of 1×10^6 cells/mL. After 48 hours (at 8% CO_2, 37°C), cells were harvested at 1500 × g for 10 minutes at 4°C and stored at −80°C. The cell pellet was thawed on ice and resuspended in lysis buffer (1xPBS, 150 mM NaCl and cOmplete EDTA-free Protease Inhibitor Cocktail (Roche)) at 5 mL/1 g of wet cell pellet. The cell suspension was then lysed by sonication on ice for 3 × 1 min at 30% amplitude, pulsing at 30 s on/30 s off. Unbroken cells and cell debris were removed via centrifugation at 3000 × *g* for 20 minutes at 4°C, followed by ultracentrifugation of the supernatant at 100 000 × *g* for 2 h. The membrane pellet was resuspended in lysis buffer (1xPBS, 150 mM NaCl, and cOmplete EDTA-free Protease Inhibitor Cocktail), flash frozen in liquid nitrogen, and stored at −80°C.

Resuspended membranes were thawed on ice and membrane proteins extracted by addition of n-dodecyl-D-maltopyranoside (DDM; Anatrace) and Cholesterol hemi succinate (CHS; Anatrace) to a final concentration of 1% (w/V) and 0.2% (w/V), respectively. The mixture was gently mixed for 1h at 4°C, followed by ultracentrifugation (100 000 ×*g*, 1 h, 4°C). The supernatant was used for subsequent purification by IMAC. Briefly, solubilized membrane proteins were incubated with Ni-NTA agarose resin in presence of 10 mM Imidazole for 1h. The beads were washed twice in wash buffer (1× PBS, 150 mM NaCl, 0.1% (w/V) DDM, and 0.02% (w/V) CHS) containing 20 mM and 40 mM Imidazole, respectively, and eluted with wash buffer containing 250 mM Imidazole. The GFP-6xHis-tag was removed by addition of TEV protease (1:1 molar ratio) overnight while dialyzing against 20 mM HEPES pH 7.5, 200 mM NaCl, 0.03% (w/V) DDM, and 0.006% (w/V) CHS. An additional IMAC step was introduced to remove the GFP-His-tag and TEV protease as well as un-cleaved protein from the suspension. The purified membrane protein was subjected to size exclusion (SEC) using a S200 10/300 increase column (GE Healthcare) equilibrated in 20 mM HEPES pH 7.5, 200 mM NaCl, 0.03% (w/V) DDM, and 0.006% (w/V) CHS. The peak fraction was subjected to an additional SEC round in the same SEC buffer. Fractions containing mMFSD1 were combined and concentrated to 0.1 mg ml^{-1}. The concentrated sample was then used for SDS-PAGE and immunoblot analysis.

2.5 | In vitro deglycosylation by Peptide -N-Glycosidase F (PNGase F)/ Endoglycosidase H (Endo H)

The cell lysates were denatured in 0.5% (w/v) SDS and 250mM ß-mercaptoethanol at 95°C for 10 minutes. The samples were adjusted to a final concentration of 12 mM EDTA, 120 mM Tris HCl pH 8.0, 1.2% (w/v) CHAPS and 2 units of PNGase F or 60 mM NaAc, 0.12% (w/v) CHAPS and 5 mU of EndoH, according to the deglycosylation reaction and incubated O/N at 37°C.

2.6 | Protein extraction and immunoblotting

Culture dishes containing cells were washed twice with PBS and 600µl of PBS supplemented with 1x complete Protease inhibitor cocktail (Roche) were added to the plate for harvesting the cells using a cell scraper. After centrifugation of the cell suspension for 8 minutes at 1000 ×*g* at 4°C, the pellet was re-suspended in lysis buffer (PBS, 1× complete and 1% (w/v) Triton X-100), sonicated twice for 20 seconds at 4°C using a Branson Sonifier 450 (level 7 in a cup horn, Emerson Industrial Automation) and lysed on ice for approximately 60 minutes (the samples were homogenized using a vortex every 15 minutes). The cell lysate was centrifuged at 16 000 ×*g* for 15 minutes at 4°C and the protein concentration of the supernatant was quantified using the Pierce BCA (bicinchoninic acid) Assay kit (Thermo Fisher Scientific) according to the manufacturer's instructions.

The protein lysates were prepared in sample buffer (125 mM Tris/HCl pH6.8, 10% (v/v) glycerol, 1% (w/v) SDS, 1% (v/v) ß-mercaptoethanol, and traces of bromophenol blue) and were denatured for 10 minutes at 55°C or 95°C depending on the hydrophobicity of the sample and its running behavior. Immunoblot was carried out according to standard procedures. After several membrane washing steps in TBS-T buffer for 10 minutes, the activity of horseradish peroxidase was detected using an ImageQuant LAS 4000 (GE Healthcare). The intensity of the signal was quantified using ImageJ software. Before incubation with new antibodies, the membranes were stripped using 0.2M NaOH. Incubations of 5 minutes at RT and gentle shaking were done in distilled water, followed by 0.2M NaOH, rinsing with distilled water, 0.2M NaOH, distilled water, and TBS-T. Next, the membranes were incubated in 5% (w/v) milk

powder in 1× TBS-T buffer for 1 hour at RT followed by incubation with the first antibody.

2.7 | Crude-membrane preparation of mouse tissues

Mouse tissues were homogenized in 10 volumes of homogenization buffer (250 mM saccharose, 10 mM Tris in PBS pH 7,4 and 1× complete inhibitor) with 10-20 strokes at 1000 rounds per minute using a Glass homogenizer (B. Braun type 853202). After centrifugation of the lysates at 1000 ×*g* at 4°C for 10 minutes the post nuclear supernatant was collected. The post nuclear supernatant was sonicated twice for 20 seconds at 4°C using a Branson Sonifier 450 (level 7 in a cup horn, Emerson Industrial Automation) and three cycles of freeze/ thaw were applied. The samples were placed into a polypropylene tube with snap-on cap (Beckmann Coulter) and ultracentrifuged at 186,000 x g in an Optima TLX Ultracentrifuge (Beckmann Coulter) using a TLA-55 rotor (Beckmann Coulter) for 1 hour at 4°C. The pellet was re-suspended in 2% SDS in PBS and the protein concentration was determined.

2.8 | Co-Immunoprecipitation

Transfected HeLa cells were lysed 48 hours post-transfection in immunoprecipitation buffer (1% CHAPS [3-[3-cholamidopropyldimethylammonio]-1-propanesulfonate] in PBS, 120 mM NaCl, 50 mM Tris HCl, 2.5 mM $CaCl_2$, 2.5 mM $MgCl_2$, and 1× complete Protease inhibitor cocktail (Roche)). Proteins were extracted and quantified as described above and 300-1000 µg of total protein were incubated with 1.5 µL of antibody O/N at 4°C in a rotor. A total of 50 µL/sample of Dynabeads Protein G per immunoprecipitation (Thermo Fisher Scientific) were blocked with 3% BSA O/N at 4°C in a rotor. Afterward, the lysate/antibody mixture was incubated with the beads for 2 hours at RT in a rotating wheel. Three washing steps of 15 minutes at RT with 1 mL immunoprecipitation buffer using a magnetic separator were applied. In a final step, the beads were incubated with 40 µL of 1× Lämmli buffer, and incubated for 10 minutes at 55°C or 95°C. Finally, the Co-IP samples were analyzed by SDS-PAGE and immunoblotting.

2.9 | Flow cytometry

Forty-eight hours after transfection, the surface expression of the indicated antigens of transfected HeLa cells was analyzed by flow cytometry. Approximately 10^6 cells were pipetted in 96-well round bottom tissue cultures plates and centrifuged at 210 ×*g* for 5 minutes at 4°C. After incubation of the samples with specific antibodies coupled to phycoerythrin (PE) diluted in MACS buffer (2 mM EDTA and 0.5% (w/v) BSA in PBS) for 45 minutes on ice in the dark, the samples were centrifuged at 210 ×*g* for 5 minutes at 4°C and washed with MACS buffer. Subsequently, the cells were centrifuged, washed again, and further re-suspended in 200 µL of MACS buffer for analysis on a FACSCanto II (BD Biosciences) device using the FACSDiva software. Positive and negative controls were used for every fluorescent dye. The data were analyzed with the FlowJo 10 software.

2.10 | Flow cytometry/ Fluorescence resonance energy transfer (FRET)

Flow cytometry was performed using a FACS Canto II (BD Bioscience). Voltage was adjusted with the BD FACSDiva software. GFP was excited with the 488 nm laser and emission was measured with a 530/30 filter; any occurring FRET signal was measured with a 670 LP filter. For each sample 30.000 events were collected. The data were analyzed with FlowJo10 software.

The indicated plasmids containing the cDNA fused to EGFP (pEGFP-N1) or mKATE2 (pmKATE2-N) in the C-terminus or EGFP (pEGFP-C1) in the N-terminus were used for transfection of HeLa cells. Forty-eight hours after transfection flow cytometry measurements were performed using a FACS Canto II (BD Biosciences) device and the results were analyzed with the FACSDiva software.

2.11 | Indirect immunofluorescence

Transfected HeLa and MEF cells grown over glass coverslips were fixed for 20 minutes with 4% (w/v) paraformaldehyde at RT, permeabilized, quenched, and blocked before incubation with primary antibodies overnight at 4°C. The samples were washed and incubated for 90 minutes with Alexa Fluor dye-conjugated secondary antibodies (Thermo Fisher Scientific). After four washing steps, the coverslips were mounted on microscope slides with mounting medium including DAPI (4-,6-diamidino-2-phenylindole) to visualize the cell nuclei. For visualization of the samples a FV1000 confocal laser scanning microscope (Olympus Life Science Solutions) equipped with a U Plan S-Apo 100× oil immersion objective (NA = 1.40) was used. Images were acquired and processed with the Olympus FluoView Software (Olympus Life Science Solutions). Single plane images for each representative image are shown throughout the manuscript.

2.12 | Statistical analyses

If not stated otherwise, two-tailed unpaired *t* test was performed using GraphPad Prism Software Version 5.03.

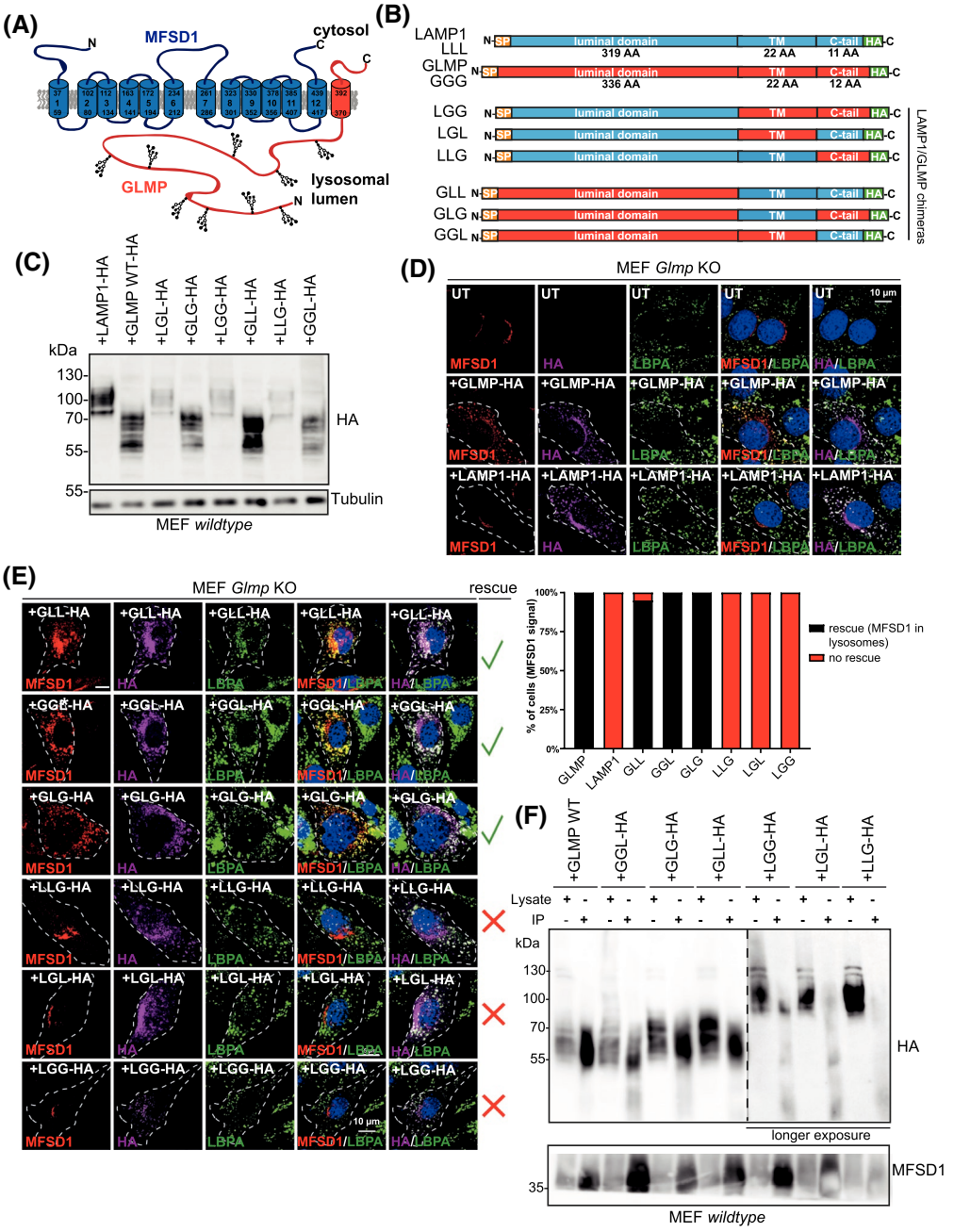

FIGURE 1 The luminal domain of GLMP interacts with MFSD1. A, Schematic representation of the molecular complex of MFSD1-GLMP. B, Schematic representation of HA-tagged chimeras of the cytosolic tail, the transmembrane domain and the luminal domain of GLMP and LAMP1. Abbreviations for the different chimeras are depicted on the left. (G = GLMP; L = LAMP1) C, Immunoblot analysis of the HA-tagged GLMP/LAMP1 chimeras expressed in wild-type MEFs detected with an antibody against HA. Tubulin is depicted as a loading control. D, Immunofluorescence staining for endogenous MFSD1 (red) in untransfected *Glmp* KO MEFs, cells transfected with GLMP-HA or LAMP1 HA (magenta). The late endosomal/ lysosomal marker LBPA is shown in green. Nuclei are stained with DAPI (blue). Transfected cells are encircled with a dashed line. UT = untransfected. E, Expression of the HA-tagged GLMP/LAMP1 chimeras (magenta) in *Glmp* KO MEFs. Endogenous MFSD1 is depicted in red. LBPA, a late endosomal lipid, is shown in green. Rescue of endogenous MFSD1 is indicated (green tick). Transfected cells are encircled with a dashed line. A quantification of the percentage of cells, in which expression of GLMP, LAMP1 or the chimeras rescues lysosomal MFSD1 is given (25-30 cells). F, Co-Immunoprecipitation of the HA-tagged GLMP/LAMP1 chimeras with MFSD1. MFSD1 was immunoprecipitated with a polyclonal antibody against MFSD1. The HA-tagged GLMP-HA, LAMP1-HA and the chimeras were detected with an antibody against HA. The right part with LGG, LGL, and LLG is shown at higher exposure, as these chimeras where expressed at lower levels. Precipitation of MFSD1 detected on the membranes with the anti-MFSD1 antibody is shown in the lower panel. (C), (D) and (E): Representative images from three independent experiments

Significant values were considered at $P < .05$. Values are expressed as mean ± standard error of the mean (SEM) and significance is designated as $*P < .05$; $**P < .01$; $***P < .001$.

3 | RESULTS

3.1 | The luminal domain of GLMP interacts with MFSD1 and is sufficient and essential for protecting MFSD1

We have shown previously that MFSD1 and GLMP form a tight protein-protein complex.[9] GLMP protects MFSD1 from lysosomal proteolysis in MEFs and MFSD1 is degraded rapidly in *Glmp* KO MEFs and *Glmp* KO mouse tissues.[9] GLMP is a lysosomal type I transmembrane protein with a short cytosolic tail, a single transmembrane domain and a highly glycosylated luminal region, similar to LAMP1 (the luminal region of LAMP1 contains two independent domains, which we, for reasons of simplicity, refer to as one "luminal domain" from here on),[15,16] (Figure 1A,B). In order to ascertain the domain(s) of GLMP that interact with MFSD1 and can rescue MFSD1 from lysosomal proteolysis in *Glmp* KO MEFs after ectopic expression, chimeric proteins of LAMP1 and GLMP were designed. cDNA chimeras coding for fusion proteins containing the different (cytosolic-, transmembrane- and luminal-) domains of GLMP (G) and LAMP1 (L) fused to an HA-tag were generated, resulting in six different chimeric proteins (Figure 1B). Overexpression of the cDNA-constructs in *wild-type* MEF cells and subsequent analysis of the lysates by immunoblot using an antibody against HA revealed that all chimeric proteins were properly expressed, though at different levels. All chimeras containing the luminal domain of LAMP1 were expressed at significantly lower level compared to those containing the luminal domain of GLMP (Figure 1C). The chimeras migrate at different molecular weight and all chimeras containing the luminal domain of LAMP1 migrated at a higher apparent molecular weight, presumably due to higher degree of glycosylation and additional polylactosaminoglycans of the luminal domain of LAMP1[17] compared to the luminal domain of GLMP (Figure 1C). Ectopic expression of the chimeras in HeLa cells revealed proper localization of all chimeras in lysosomes and barely any cells with misfolded chimeric proteins in the ER (Supplemental Figure 1A). Ectopic expression of MFSD1 in HeLa cells alone results in the generation of C- and N-terminal fragments (C-/ NTFs). Co-expression of GLMP prevents the generation of these fragments.[9] We used this experimental setup for testing if the chimeric proteins can prevent the generation of the N-terminal fragment of MFSD1. Co-expression of full length GLMP and all chimeras containing the luminal domain of GLMP quantitatively prevented the generation of the NTF of MFSD1, but co-expression of full length LAMP1 or chimeras containing the luminal domain of LAMP1 did not (Supplemental Figure 1B). However, the interpretation of the data was challenged by the lower expression of the chimeras containing the luminal domain of LAMP1. We, therefore, changed to an imaging-based experimental setup, in which we compared cells with comparable expression of each chimera. Endogenous MFSD1 is strikingly reduced in *Glmp* KO MEFs and residual MFSD1 is found in the Golgi apparatus (Figure 1D,[9]). While the re-introduction of HA-tagged GLMP into GLMP-deficient MEFs efficiently rescues the lysosomal localization of endogenous MFSD1, the overexpression of LAMP1-HA is not affecting the levels and mislocalization of MFSD1 (Figure 1D). After transfection of *Glmp* KO MEFs with cDNA coding for the six different HA-tagged GLMP-LAMP1 chimeras followed by immunofluorescence staining, we observed that only the constructs containing the luminal domain of GLMP (GGL, GLG, and GLL) rescued the lysosomal localization of MFSD1 (Figure 1E). The introduction of the chimeras containing the luminal domain of LAMP1 (LGG, LGL, and LLG) in GLMP-deficient MEFs did not recover the lysosomal localization of MFSD1. It should be noted that we selected cells with equal expression of the constructs for microscopy, precluding bias due to the overall lower expression of the chimeras containing the luminal domain of LAMP1 (Figure 1C). These results suggest that the luminal domain of GLMP is essential but also sufficient for rescuing MFSD1. Next, we tested by co-immunoprecipitation which of the different HA-tagged GLMP-LAMP1 chimeras physically interact with MFSD1. After transfection and immunoprecipitation of MFSD1 with the anti-MFSD1 antibody, only the chimeric proteins containing the luminal domain of GLMP were efficiently co-immunoprecipitated (Figure 1F). These results are in agreement with the immunofluorescence-based rescue experiments (Figure 1E), corroborating the finding that the luminal domain of GLMP physically interacts with MFSD1 and that it is indispensable for the lysosomal localization and rescue of MFSD1 in *Glmp* KO MEFs.

3.2 | The stability of GLMP depends on N-glycosylation

Because the luminal domain of GLMP is highly N-glycosylated and MFSD1 is not glycosylated,[9,15] it is tempting to speculate that N-glycosylation of GLMP protects MFSD1 from lysosomal proteolysis. We, therefore, addressed the question if the type of N-glycosylation (complex-type vs high-mannose-type) of GLMP was important for the rescue of MFSD1. GLMP-deficient MEFs were transfected with GLMP-HA and treated with kifunensine, an inhibitor of the ER mannosidase I,[11] preventing the addition of any complex-type N-glycosylation. Kifunensine-treatment resulted

in a much more homogeneous N-glycosylation pattern of GLMP, observed as a sharp band, compared to untreated cells, which displayed a diffuse fuzzy band as assessed by immunoblot (Figure 2A). Digestion of lysates of kifunensine-untreated cells with the high-mannose type-specific glycosidase Endo-β-N-acetylglucosaminidase H (EndoH) caused only a marginal shift in the apparent molecular weight of GLMP, while N-glycosidase F (PNGaseF), cleaving both high-mannose-type and complex-type N-glycans, reduced the apparent molecular weight almost to the predicted molecular weight of ~43 kDa, indicating that GLMP is normally almost exclusively equipped with complex-type N-glycans. These findings are in agreement with previous results.[15] It should be noted that under these conditions, GLMP was likely not fully deglycosylated, resulting in a blurry banding pattern. More extensive deglycosylation resulted in a loss

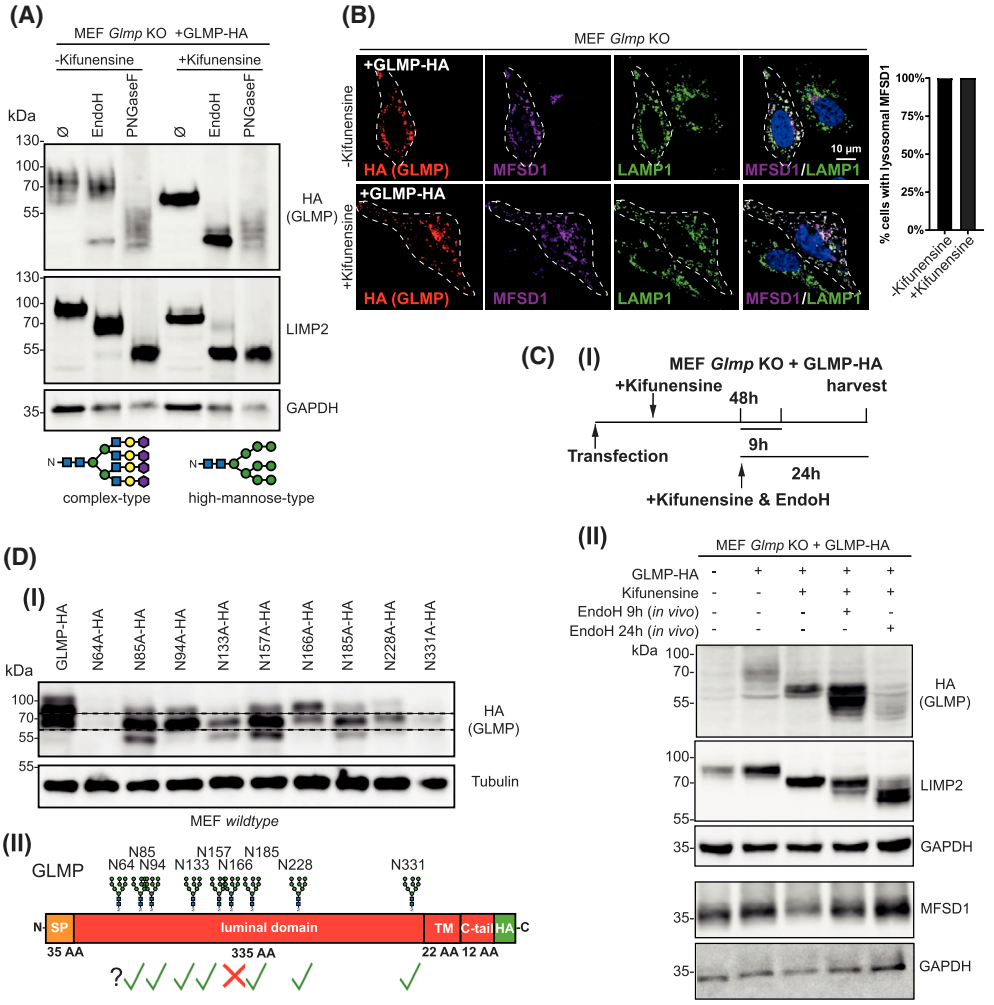

FIGURE 2 High-mannose type N-glycosylated GLMP can rescue MFSD1. A, Immunoblot analysis with the anti-HA antibody of *Glmp* KO MEF transfected with HA-tagged GLMP untreated or treated in vivo with the mannosidase I inhibitor kifunensine. Cell lysates were treated in vitro with EndoH or PNGaseF. LIMP2, which contains both high-mannose-type and complex-type glycans is shown as a positive control for the kifunensine-, EndoH-, and PNGaseF-treatment. GAPDH is depicted as a loading control. The N-glycan structures of complex-type glycans (left) and high-mannose-tye glycans (right), the latter resulting from kifunensine-treatment, are schematically depicted below the immunoblot (blue square = N-Acetyl-D-glucosamine; green circle = mannose; yellow circle = galactose; magenta hexagon = neuraminic acid). B, Immunofluorescence for endogenous MFSD1 (purple) in *Glmp* KO MEFs transfected with GLMP-HA (red). Cells were untreated or incubated in vivo with kifunensine. The lysosomal marker LAMP1 is depicted in green. Nuclei are stained with DAPI (blue). Transfected cells are encircled with a dashed line. The percentage of cells with lysosomal MFSD1 staining pattern is diagramed (35-40 cells). C, (I) Schematic representation of the kifunensine/EndoH in vivo experimental setup. (II) Immunoblot analysis of GLMP-deficient MEFs transfected with HA-tagged GLMP untreated or treated with kifunensine and EndoH with the anti-HA antibody. LIMP2 is shown as a positive control for the kifunensine- and EndoH-treatment. Endogenous MFSD1 was detected with an MFSD1-specific antibody. GAPDH is depicted as a loading control. D, (I) Immunoblot analysis of *wild-type* MEFs overexpressing GLMP-HA or GLMP-HA with N/A mutations in the nine putative N-glycosylation sites detected with the anti-HA antibody. (II) Schematic representation of N-glycosylated asparagine residues in the luminal domain of GLMP. (A)-(C): Representative images from three independent experiments

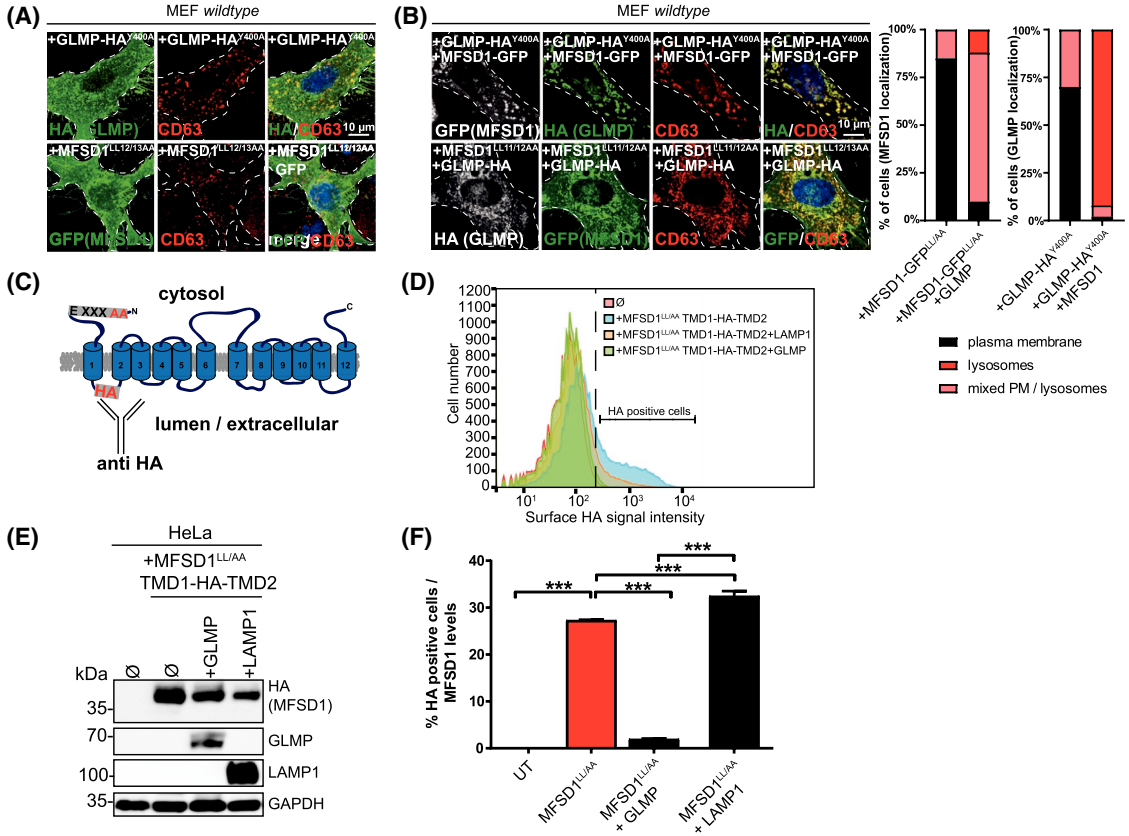

FIGURE 3 GLMP can deliver plasma-membrane targeted MFSD1 to lysosomes and *vice versa*. A, Immunofluorescence analysis of wild-type MEFs expressing GLMP$^{Y/A}$-HA mutant (green) or MFSD1$^{LL/AA}$-GFP mutant (green) co-stained with the lysosomal marker CD63 (red). Nuclei are stained with DAPI (blue). Transfected cells are encircled with a dashed line. B, Immunofluorescence analysis of MEFs expressing GLMP$^{Y/A}$-HA mutant (green) together with MFSD1-GFP (white) or MFSD1$^{LL/AA}$-GFP mutant (green) together with GLMP-HA (white) co-stained with the lysosomal marker CD63 (red). Nuclei are stained with DAPI (blue). Transfected cells are encircled with a dashed line. (A) - (B): Representative images from three independent experiments. The number of cells with MFSD1$^{LL/AA}$-GFP/ GLMP$^{Y/A}$-HA at the plasma membrane, plasma membrane and lysosomes (mixed) or lysosomes is depicted (n = 30-40 cells). C, Schematic representation of the MFSD1$^{LL/AA}$-construct with an internal-HA-tag between TMD 1 and 2 (MFSD1$_{int}^{LL/AA}$) used for FACS analysis. D, FACS plots of untransfected HeLa cells, cells transfected with MFSD1$_{int}^{LL/AA}$ alone or together with LAMP1 or GLMP after staining of HA without permeabilization. E, Immunoblot analysis of untransfected HeLa cells, cells transfected with the MFSD1$_{int}^{LL/AA}$ alone or together with LAMP1 or GLMP, respectively. F, Quantification of the percentage of HA positive cells shown in (D) normalized to the HA expression levels shown in (E) (two-tailed unpaired *t* test; Mean ± SEM, n = 5. ***$P < .0001$)

of immunoreactivity by immunoblot (not shown). Digestion of lysates of kifunensine-treated MEFs with EndoH resulted in complete deglycosylation of GLMP-HA, indicating that GLMP-HA is quantitatively equipped with high-mannose type N-glycosylation upon kifunensine treatment. Re-introduction of GLMP-HA in kifunensine-treated *Glmp* KO MEFs (ie, GLMP equipped with high-mannose type glycans) rescued the endogenous MFSD1 lysosomal localization, suggesting that the type of N-glycosylation (high-mannose-type or complex-type) of GLMP is not critical for the interaction and protection of MFSD1 (Figure 2B). Next, we addressed whether non-glycosylated GLMP could rescue MFSD1 in *Glmp* KO MEFs. For that purpose, a GLMP cDNA with mutations of the critical asparagine residue to alanine in its previously described nine putative N-glycosylations sites[15] was transfected into GLMP-deficient MEFs. However, this mutant was quantitatively retained in the ER, most likely due to misfolding (data not shown). To overcome the aberrant protein folding and quality control in the ER, we treated GLMP-deficient MEFs overexpressing wild-type GLMP-HA with kifunensine and EndoH in vivo. EndoH is efficiently endocytosed and active at the acidic pH of lysosomes, therefore, resulting in in vivo deglycosylation of lysosomal high-mannose type glycosylated proteins.[18] In vivo deglycosylation affects lysosomal membrane proteins to a different extent: whereas deglycosylation of LAMP1 and LAMP2 leads to their rapid degradation, the stability of another highly glycosylated lysosomal membrane protein (LIMP2) is not affected.[18] We next tested the effect of in vivo deglycosylation on GLMP. We offered EndoH to the cells for different time points. In vivo treatment of high-mannose type glycosylated GLMP for 24 hours with EndoH (Figure 2C) leads to the degradation of GLMP as determined by immunoblot for the HA-tag, indicating that GLMP stability depends on N-glycosylation, similar

to the LAMP-proteins.[18] Surprisingly, the levels of MFSD1 did not follow the same decrease as GLMP (Figure 2C), indicating that either the degradation follows a slower kinetic, or that not only protection of MFSD1 by GLMP influences its levels, but also other factors like effects on intracellular sorting. Since N-glycosylation is critical for the stability of GLMP, we analyzed which of the nine putative N-glycosylation sites are occupied/critical (Figure 2D). All potential N-glycosylation sites (with the motif N-X-S/T) were tested individually by mutating the corresponding asparagine residue (N) to alanine (A). The kifunensine treatment of cells after overexpression of the GLMP mutants resulted in three sharp bands that allowed the discrimination of small molecular weight differences (Figure 2D). N64A was expressed at very low levels and even with high exposure (Supplemental Figure 1A), no definitive conclusions could be drawn. While the apparent molecular weight of the N166A GLMP mutant was not decreased, the seven remaining GLMP N/A-mutants had an apparent molecular weight of approximately 3 kDa smaller than wild-type GLMP, indicating that N-glycans are attached to those asparagine-residues in wild-type GLMP (Figure 2D and Supplemental Figure 2A). Next, we tested by immunofluorescence analysis whether the introduction of GLMP N-glycosylation mutants in *Glmp* KO MEFs still rescues endogenous lysosomal MFSD1 (Supplemental Figure 2B). Interestingly, overexpression of all GLMP mutants harboring mutation of a s single N-glycosylation site in GLMP-deficient MEFs was able to rescue lysosomal localization of MFSD1, indicating that not a single N-glycan confers protection for MFSD1, but the sum or at least more than one N-glycan. In summary, these data support a protective function of GLMP on MFSD1 and particularly a protective function of N-glycosylation on GLMP itself.

3.3 | The MFSD1-GLMP interaction overcomes the cell surface mislocalization of $GLMP^{Y/A}$ and $MFSD1^{LL/AA}$ mutants

The interaction between transporters and their corresponding accessory subunits often affects the intracellular transport of the complex. This is for instance the case for CLC-7, a lysosomal chloride transporter, and OSTM1, its β-subunit that shows an ER-like distribution when overexpressed alone, but lysosomal localization when co-expressed with CLC-7.[6] We have shown previously that ectopically overexpressed MFSD1 and GLMP can reach lysosomes in the absence of their corresponding interaction partners in KO MEFs for the corresponding genotype.[9] Both MFSD1 and GLMP exhibit dileucine or tyrosine-based sorting motifs in their cytosolic N- and C-termini, respectively (Supplemental Figure 3A,[9,15]). Mutation of these sorting motifs followed by ectopic expression in cells lead to the localization to the cell surface of both *GLMP*$^{Y/A}$ and *MFSD1*$^{LL/AA}$ mutants ([9] Figure 3A). The highly stable interdependence of GLMP and MFSD1 suggests a strong interaction. Therefore, we studied whether the co-expression of cell surface mutants of MFSD1 or GLMP ($MFSD1^{LL/AA}$ or $GLMP^{Y/A}$) together with wild-type GLMP or MFSD1, respectively, would change the subcellular localization of the proteins. Immunofluorescence analysis of MEF cells after co-transfection with either $GLMP^{Y/A}$-HA and MFSD1-GFP or $MFSD1^{LL/AA}$-GFP and GLMP-HA revealed co-localization of $GLMP^{Y/A}$-HA and $MFSD1^{LL/AA}$-GFP with the lysosomal marker CD63, indicating proper delivery to lysosomes despite mutation of the respective sorting motifs and differing from overexpression of the $GLMP^{Y/A}$-HA and $MFSD1^{LL/AA}$-GFP alone (Figure 3B). However, while $GLMP^{Y/A}$-HA was nearly absent from the cell surface when co-expressed with wild-type MFSD1-GFP, $MFSD1^{LL/AA}$-GFP could still be partially observed at the cell surface after co-transfection with GLMP-HA. To obtain quantitative data, $MFSD1^{LL/AA}$ with an internal HA-tag (designated as $MFSD1_{int}^{LL/AA}$) between transmembrane domain (TMD)1 and TMD2 (Figure 3C,[9]), was co-expressed in HeLa cells together with GLMP or together with LAMP1 (as a negative control) and the cell surface levels of MFSD1 were analyzed by flow cytometry. These experiments showed that $MFSD1_{int}^{LL/AA}$ was barely present at the cell surface after co-expression with GLMP, while after co-expression of LAMP1 large amounts of $MFSD1_{int}^{LL/AA}$ were still detected at the plasma membrane (Figure 3D-F, Supplemental Figure 3A-C). For normalization of the FACS results on the MFSD1-protein levels, immunoblots for MFSD1, GLMP, and LAMP1 were performed in replicates (Supplemental Figure 3B). A representative blot is shown in (Figure 3E). Quantification of the FACS data in replicates, normalized to the HA expression levels determined by immunoblot, showed significantly lower $MFSD1_{int}^{LL/AA}$ -surface levels after co-expression of GLMP compared to co-expression with LAMP1 or expression of $MFSD1_{int}^{LL/AA}$ alone (Figure 3F). These results illustrate that the interaction between MFSD1 and GLMP can partially redirect $GLMP^{Y/A}$ or $MFSD1^{LL/AA}$ to lysosomes when co-expressed with MFSD1 or GLMP, respectively, and indicate that the interaction of MFSD1-GLMP occurs in earlier subcellular compartments than lysosomes. Moreover, these data pinpoint, that the interaction of GLMP and MFSD1 is not only important for stability but also affects the intracellular sorting of the two proteins.

3.4 | MFSD1 interacts with GLMP already in the ER

We next tested if the two proteins already start to interact in the ER. To that end, a sequence coding for the C-terminal ER-retention signal of the human α2C adrenergic receptor[19]

was fused to the C-terminus of MFSD1-HA (MFSD1$^{ER\ Ret}$-HA) to retain MFSD1 in the ER (Figure 4A). Immunofluorescence analysis of MEF cells overexpressing MFSD1$^{ER\ Ret}$-HA showed no co-localization of this artificial fusion protein with the lysosomal marker LAMP1, but extensive co-localization with the ER-marker PDI and less co-localization with the *cis*-Golgi marker GM130, respectively (Figure 4B). Overexpression of MFSD1 alone, but not together with GLMP, leads to proteolytic fragmentation due to lysosomal proteolysis.[9] We used the formation of the fragments as an additional readout for the lack of delivery to late endocytic organelles. Immunoblot analysis with MFSD1- and HA-antibodies of HeLa cells overexpressing MFSD1$^{ER\ Ret}$-HA showed a strong reduction in the ratio of both C- and N-terminus/Full length of MFSD1$^{ER\ Ret}$-HA when compared to MFSD1-HA, supporting the immunofluorescence data that MFSD1$^{ER\ Ret}$-HA is not reaching lysosomes (Figure 4C).

To test whether MFSD1 and GLMP interact in earlier subcellular compartments than lysosomes, MFSD1$^{ER\ Ret}$-HA was co-expressed with GLMP or LAMP1 fused to mKATE2 and the subcellular localization was analyzed by immunofluorescence. While MFSD1$^{ER\ Ret}$-HA did not reach lysosomes after co-expression with LAMP1-mKATE2, as indicated by co-staining with the lysosomal marker CD63, the overexpression of MFSD1$^{ER\ Ret}$-HA together with GLMP-mKATE2 lead to a clear co-localization of MFSD1$^{ER\ Ret}$-HA with CD63 (Figure 4D). No co-localization of MFSD1$^{ER\ Ret}$-HA with the ER and *cis*-Golgi markers PDI and GM130 was detected after co-expression with GLMP-mKATE2 (Supplemental Figure 4A,B). These results suggest that the complex composed of MFSD1 and GLMP is already formed in the ER and that the sorting of the two interaction partners is strong enough to overcome the α2C adrenergic receptor-ER retention motif of MFSD1$^{ER\ Ret}$-HA. Additionally, these data highlight again, that the interaction of the two proteins can affect their intracellular trafficking.

3.5 | MFSD1 and GLMP levels quantitatively depend on each other

Immunoblot analysis showed that MFSD1 levels are decreased to less than 5% in different tissues of *Glmp* KO mice compared to *wild-type* mice, similar to GLMP levels in *Mfsd1* KO tissues.[9] Ectopic expression of MFSD1 in HeLa cells alone results in the generation of C- and N-terminal

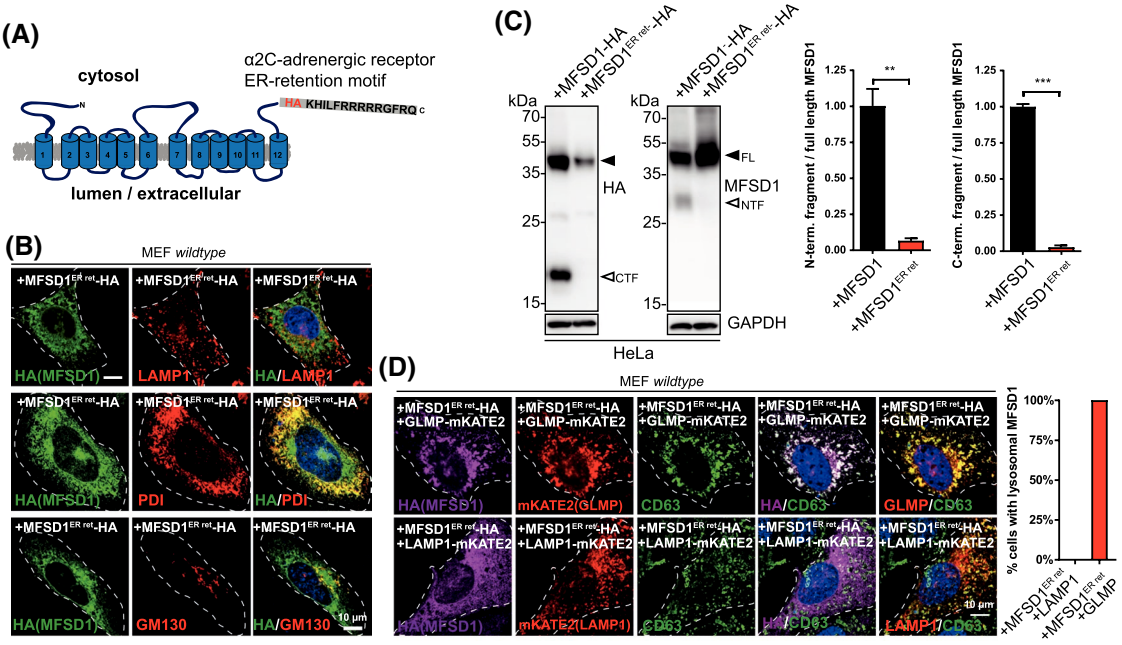

FIGURE 4 GLMP and MFSD1 interact already in the ER. A, Schematic representation of a MFSD1-HA construct fused C-terminally to the α2C-adrenergic receptor ER-retention motif (MFSD1$^{ER\ Ret}$-HA). B, Immunofluorescence analysis of MEFs expressing the MFSD1$^{ER\ Ret}$-HA construct (green) co-stained with the lysosomal marker LAMP1 (red), the ER marker PDI (red) or the *cis*-Golgi marker GM130 (red). Nuclei are stained with DAPI (blue). Transfected cells are encircled with a dashed line. C, Immunoblot analysis of HeLa cells overexpressing MFSD1-HA or MFSD1$^{ER\ Ret}$-HA with antibodies against MFSD1 and HA. The full-length (FL) MFSD1 is labeled with a black arrowhead, the N- and C-terminal fragments (NTF and CTF, respectively), are labeled with an open arrowhead. Quantification of the rate of the N- and C-terminal fragments/Full length MFSD1 is depicted (two-tailed unpaired *t* test; Mean ± SEM, n = 3. ***$P < .0001$; **$P < .01$; n = 2). (D) Immunofluorescence analysis of MEFs transfected with MFSD1$^{ER\ Ret}$-HA stained for HA (purple) together with GLMP-mKATE2 or LAMP1-mKATE2 (red) and co-stained with the lysosomal marker CD63 (green). Nuclei are stained with DAPI (blue). Transfected cells are encircled with a dashed line. Representative images from three independent experiments. The percentage of cells with lysosomal MFSD1 staining pattern is depicted (35-40 cells)

fragments (C-/ NTFs) and co-expression of GLMP prevents the generation of these fragments.[9] These data indicate that both proteins of the complex are essential for maintaining their stability. Next, we addressed the question, if both proteins quantitatively depend on each other. For this, a constant MFSD1 cDNA concentration was transfected in HeLa cells with increasing and decreasing amounts of GLMP and LAMP1 cDNAs, respectively, and the ratio of CTF/full-length MFSD1 was determined. Immunoblot analysis of the cell lysates using HA-, GLMP-, and LAMP1-specific antibodies revealed that the CTF/FL MFSD1 ratio was inversely proportional to the GLMP expression levels (Figure 5A), implicating a quantitative interdependency of the two subunits. We then tested whether the levels of GLMP also quantitatively depend on MFSD1 levels in vivo. Therefore, membrane fractions of kidney, liver, lung, and spleen from wild type, heterozygous or knockout for *Mfsd1* were analyzed by immunoblot with antibodies against MFSD1, GLMP, and CoxIV (as a membrane-protein loading control) (Figure 5BI). These experiments indicate that in all four tissues from *Mfsd1* heterozygous mice, the levels of GLMP were reduced to approximately half when compared to wild-type tissues. These differences reached statistical significance for liver and spleen (Figure 5BII). Altogether, these findings indicate that both, GLMP and MFSD1 stability quantitatively depend on the direct interaction with their corresponding interaction partner, and once one of the partners of the complex is limiting, this ultimately leads to the rapid degradation of the other partner.

3.6 | MFSD1 can form homodimers

Several transporter proteins, including members of the MFS-family form heterodimers and/or homodimers (reviewed in 20). For instance, a member of the MFS transporter family, MCT8, forms dimers resistant to denaturation and reducing conditions.[21] We, therefore, analyzed if MFSD1 can form oligomers. After ectopic expression of MFSD1-HA in HeLa cells we consistently observed by immunoblot analyses an additional band at ~70 kDa, approximately at the double size of full-length MFSD1, suggesting that MFSD1 might also form dimers partially resistant to denaturing conditions and β-mercaptoethanol (Figure 6A). It is unlikely that the observed band resembles the complex between MFSD1 and GLMP, given the apparent molecular weight of GLMP

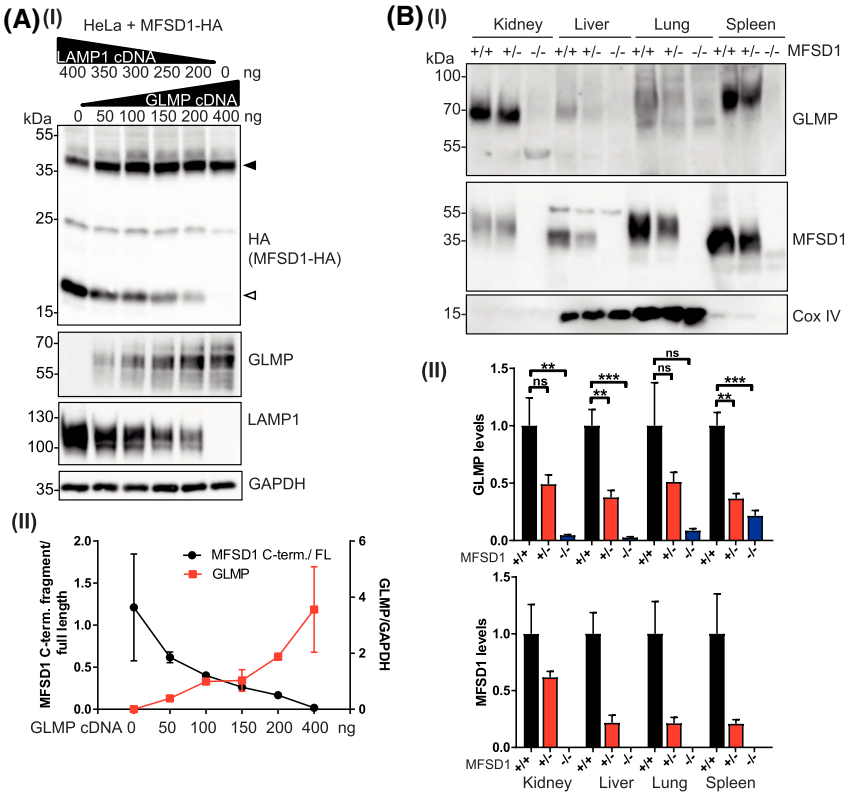

FIGURE 5 MFSD1 levels quantitatively depend on GLMP levels and *vice versa*. A, (I) Immunoblot analysis of HeLa cells overexpressing MFSD1-HA together with decreasing amounts of LAMP1 cDNA and increasing amounts of GLMP cDNA detected with HA, GLMP and LAMP1 antibodies. GAPDH is shown as a loading control. (II) A quantification of the ratio C-terminal/Full length MFSD1 and of the GLMP levels is represented (n = 3). B, (I) Immunoblot analysis of MFSD1 wild type, heterozygous, and homozygous knockout kidney, liver, lung, and spleen membrane fractions with anti-MFSD1 and anti-GLMP antibodies. CoxIV is shown as a loading control. (II) Quantification of MFSD1 and GLMP levels in the different tissues normalized by the levels of CoxIV. (two-tailed unpaired *t* test; Mean ± SEM, n = 3-4.$^{**}P < .01$$^{***}P < .001$)

alone is ~70 kDa. To specifically investigate if MFSD1 forms homodimers, we performed co-immunoprecipitation assays using MFSD1 constructs fused to eGFP- or HA-tags. MFSD1-HA and MFSD1-eGFP were efficiently co-immunoprecipitated with MFSD1-eGFP or MFSD1-HA, respectively, from HeLa cells transfected with both MFSD1-eGFP and MFSD1-HA constructs (Figure 6B). MFSD1-HA was efficiently detected in GFP-precipitates and MFSD1-GFP was efficiently co-precipitated in HA-precipitates, indicating physical interaction between the differentially tagged MFSD1 proteins. To rule out unspecific co-immunoprecipitation due to the use of CHAPS as a detergent, the presence of another lysosomal membrane protein, LIMP2, in the immunoprecipitated fraction was analyzed. The result showed no LIMP2 band in the immunoprecipitated fractions, indicating specific immunoprecipitation.

Attempts to purify ectopically expressed recombinant MFSD1 (recMFSD1) from HEK293F cells by Ni-NTA affinity chromatography followed by size exclusion chromatography revealed a monodisperse elution profile. RecMFSD1 eluted earlier from the size exclusion column than a known monomeric membrane transporters of similar size, indicative for a higher oligomeric assembly or an increased amount of lipids and detergents bound to purified MFSD1 (Supplemental Figure 5A). Immunoblot analysis of recMFSD1 revealed, as seen before by immunoblot analysis

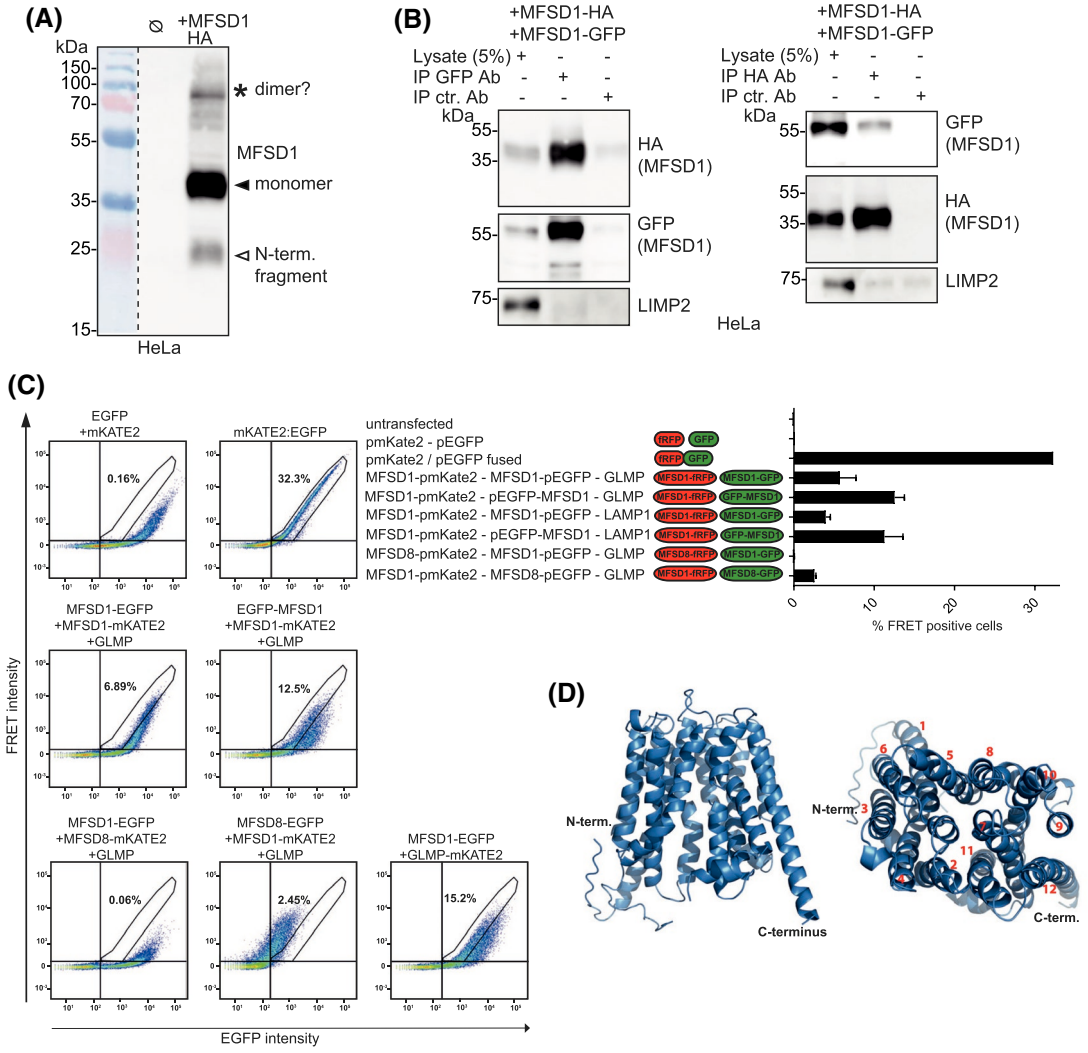

FIGURE 6 MFSD1 can form homodimers. A, Immunoblot analysis of HeLa cells overexpressing MFSD1-HA with an anti-HA antibody. A putative dimer is labeled with an asterisk. B, Immunoprecipitation of MFSD1-HA and MFSD1-GFP from transfected HeLa cells lysates transfected with both constructs using antibodies against HA and GFP. Co-immunoprecipitated proteins are detected with anti-HA and anti-GFP antibodies. Representative images from 2-3 independent experiments. C, Flow cytometry-based FRET analysis of HeLa cells transfected with combinations of plasmids coding for MFSD1, GLMP and MFSD8 untagged or tagged with eGFP or mKATE2. FRET intensity is plotted against eGFP intensity. Cells inside the gate defined by the intensity of cells expressing fused eGFP:mKATE2 were considered FRET+. The given numbers in the plot represents the average of alive FRET + cells for each condition, which is also represented in the bar graph. n = 3/ condition. D, Structure prediction of mMFSD1 using Phyre2 software with GLUT3 as a model. The prediction covers the mMFSD1 amino acid sequence from S20 to S451. Numbers in red represent the TMDs (1 = most N-terminal TMD, 12 most C-terminal TMD)

of lysates from transfected cells, bands at ~70 kDa presumably corresponding to a dimer (Supplemental Figure 5B).

Additionally, we validated dimer formation of MFSD1 with an independent approach by FACS-based Förster resonance energy transfer (FRET) (Figure 6C). We used the green fluorescent protein eGFP and the red fluorescent protein mKATE2 for generating fusion proteins, a combination that was shown previously to yield efficient FRET,[9,10] as FRET couple. MFSD1 was fused to eGFP at the C- or the N-terminus (MFSD1-eGFP and eGFP-MFSD1) and to mKATE2 at its C-terminus (MFSD1-mKATE2). As a negative control, the polytopic lysosomal transporter MFSD8 was used in the experimental setup. HeLa cells transfected with a fusion protein between eGFP and mKATE2 (eGFP:mKATE2) were used as a positive control for FRET. The eGFP-fusion proteins were expressed to a similar extent in all samples (Supplemental Figure 4C). To test whether GLMP influences MFSD1 homodimerization, GLMP, or LAMP1, as a negative control, were co-expressed together with mKATE2- and eGFP-tagged MFSD1 (Figure 6D, Supplemental Figure 4C). While MFSD1-mKATE2 did not show efficient FRET with MFSD1-eGFP, FRET was occurring between MFSD1-mKATE2 and eGFP-MFSD1 suggesting that the MFSD1 C-terminus is close to the N-terminus of the dimerization partner molecule. Additionally, the co-expression of GLMP did not increase MFSD1 homodimerization. Co-expression of MFSD1-FRET constructs and LAMP1 yielded a similar FRET signal intensity compared to co-expression with GLMP, indicating that GLMP is dispensable for homodimerization of MFSD1. These results are in line with the previous co-immunoprecipitation experiments and indicate that MFSD1 can form homodimers. GLMP is dispensable for this homodimerization. In summary, our experiments indicate that MFSD1 is not present per se in an oligomeric state but can form homodimers.

4 | DISCUSSION

We have shown previously that the two lysosomal integral membrane proteins MFSD1 and GLMP form a tight complex.[9] In this study, we refined the molecular interaction of the two proteins and found the luminal domain of GLMP alone, but not its transmembrane domain or the short cytosolic tail confers protection and interaction with MFSD1. Our data support the finding that the protein-protein interaction is essential for stabilization of the two proteins in a complex and that N-glycosylation is essential for this process.

We investigated which domain of GLMP interacts with MFSD1 and found the luminal domain to be critical. In this regard, GLMP and MFSD1 deviate from other couples of transporters and their corresponding type I-topology accessory subunits like CLCN-7 and OSTM1.[22] In OSTM1, the transmembrane domain was shown to be necessary and sufficient for OSTM1 constructs being carried to lysosomes by CLCN-7, and both the transmembrane and the luminal domain are needed for proper H+/Cl− exchange of CLCN-7.[22] These differences might reflect differences in the major function of the accessory subunits and their corresponding transporter: The major function of OSTM1 is to facilitate trafficking of CLCN-7 and H+/Cl− exchanger function, while the major function of GLMP is likely the protection of MFSD1 from lysosomal proteases, though trafficking is apparently also part of the shared interaction, at least under abnormal conditions when MFSD1 is missorted to the plasma membrane. In this line, we further investigated the effect of altered N-glycosylation of GLMP on its protective function of MFSD1. Our results implicate, that (1) GLMP needs to be equipped with N-glycans, for not being degraded by lysosomal proteases itself and hence, that N-glycosylation is indirectly necessary for protecting MFSD1 and (2) not a single N-glycan directly confers protection of GLMP (and indirectly MFSD1) or an interaction of a single glycan with MFSD1, but the sum of N-glycans shields GLMP. If the luminal domain is also essential for the transporter activity of MFSD1 can only be determined once its substrate is known and a transporter assay is established. Our chimeras will be a useful tool to analyze a possible contribution of GLMP to the transporter function of MFSD1 once such assays are available.

Even though several lines of evidence support the protective effect of GLMP on MFSD1 and *vice versa* ([9] Figure 2), we considered the possibility that the two proteins additionally reciprocally affect their intracellular sorting. Furthermore, we wanted to figure out, whether the interaction starts in the ER, the Golgi-apparatus or even in late endosomes/lysosomes. Surprisingly, the co-expression of wild-type GLMP was able to overcome the ER-retention of MFSD1. Of note, $MFSD1^{ER\ ret}$ did not retain GLMP in the ER. These data suggest that (1) the two proteins already assemble into a complex in a pre-Golgi-compartment and most likely in the ER, and (2) that the formation of the complex triggers their translocation to lysosomes, implicating an effect on the intracellular transport. The findings of these experiments were additionally supported by showing that co-expression of wild-type MFSD1 or wild-type GLMP with mutations in their respective sorting motifs lead to proper localization to lysosomes instead of the plasma membrane. This finding can be explained by two possible scenarios: either the sorting-motif-mutated protein ($MFSD1^{LL/AA}$ or $GLMP^{Y/A}$, respectively), and its wild-type counterpart are transported together directly from the Golgi apparatus via endosomes to lysosomes (Figure 7A), and an intact sorting motif of one of the partners is sufficient to maintain normal intracellular delivery. The other possibility is that both proteins take, to some extent, the indirect pathway for their delivery to lysosomes via the plasma membrane (Figure 7B), and the two proteins are transported in

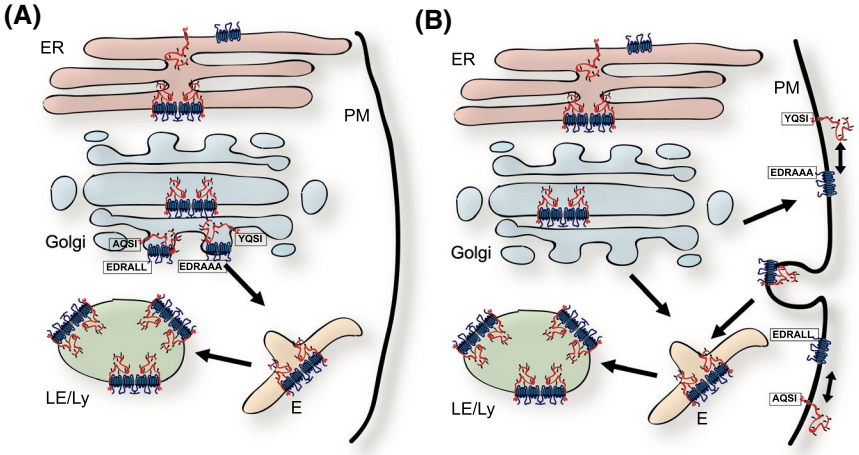

FIGURE 7 Schematic summary of the findings of this study. The interaction between MFSD1 and GLMP starts in the ER. MFSD1 forms dimers. Plasma-membrane missorted MFSD1 containing mutations in the dileucine-based sorting motif (EDRALL) (the critical amino acids are underlined) to EDRAAA is either re-endocytosed upon GLMP WT co-expression (B) or directly transported from the TGN to lysosomes (A). Plasma membrane missorted GLMP containing a mutation in the tyrosine-based sorting motif (YQSI) to AQSI is either re-endocytosed upon MFSD1 WT co-expression (B) or directly transported from the TGN to lysosomes (A)

a complex from the plasma membrane via endocytosis and AP-2 to lysosomes. In this regard, it should be noticed that tyrosine-based sorting motifs are preferentially found in proteins that are destined for endocytosis from the plasma membrane.[23] The latter possibility would also offer an interesting mechanistic explanation: missorted MFSD1 (or GLMP) might be toxic for cells in vivo (however, we found no evidence that either $MFSD1^{LL/AA}$ or $GLMP^{Y/A}$ overexpression is toxic) and re-endocytosis via MFSD1/ GLMP is a protective mechanism, or this could be a kind of back-up system for efficient delivery to lysosomes even if MFSD1 or GLMP are partially missorted to the plasma membrane.

We finally analyzed the interdependence of MFSD1 and GLMP quantitatively and provide evidence that MFSD1 can form homodimers both in vitro and in vivo. Whether dimerization is critical for its function needs to be clarified in future experiments. Although we cannot fully rule out postlytic artificial dimerization in vitro, the combination of in vivo and in vitro data suggests that this oligomerization is a true biological finding. Notably, oligomerization is well documented for several members of the MFS, mainly affecting the transporter activity. In this regard, oligomerization may play a regulatory role. Reduced oligomerization leading to increased transport activity (V_{max}) has been documented for other members of the MFS family including the plant phosphate transporter, Pht1,[24] and the plant nitrate transporter NRT1.1.[25] Once a substrate for MFSD1 can be identified, this will be an important question to be addressed. The general folding of MFS proteins is well preserved and we, therefore, predicted the structure of MFSD1 using Phyre2 software with GLUT3 as a model (Figure 6D). Interestingly the FRET couple with C-terminally tagged mKATE2 and N-terminally tagged EGFP yielded higher FRET compared to C-terminally tagged mKATE2 and C-terminally tagged EGFP, indicating that the interaction likely occurs at the interface between the long C-terminal helix and the cytosolic N-terminal tail.

Interestingly, the expression of both MFSD1 and GLMP seem to be closely balanced, because a lack of sufficient amounts of one of the interaction partners leads to a linear decrease of the other interaction partner. These experiments suggest that the expression of both proteins must be highly regulated so that both are expressed in an equimolar ratio, or that GLMP is expressed in excess so that it is not limiting. Such an excess of GLMP could ensure quantitative delivery of MFSD1 to lysosomes. The stoichiometry (ie, if more than one molecule of one subunit is interacting with the other partner) of other couples of lysosomal membrane complexes (eg, CLCN-7 and OSTM1,[26] SLC37A3 and ATRAID[8] or ABCD4 and LMBD1[10]) and even the possibility of homodimerization of the transporting subunit has not yet been determined. It will be interesting in future studies, how these interacting-couples are regulated and if, similar to MFSD1 and GLMP, one of the interaction partners is limiting. This is particularly interesting for the disease-causing proteins like CLCN-7, OSTM1, and ABCD4/LMBD1, given that heterozygote mutations could already have a deleterious effect on the levels and possibly function of the other interacting subunit.

ACKNOWLEDGMENT

We thank Maike Langer and Sebastian Held for excellent technical assistance. Winnie Eskild is acknowledged for the gift of *Glmp* knockout MEFs. Stephan Storch and Sean Froese are acknowledged for the gift of plasmids. Paul Saftig is acknowledged for critical reading of the manuscript, discussion, and ongoing support. This work was in part supported by the Deutsche Forschungsgemeinschaft (DFG) to MD (DA 1785-1). The authors declare no financial and nonfinancial

competing interests. Open access funding enabled and organized by Projekt DEAL.

CONFLICTS OF INTEREST

The authors declare no conflict of interest or competing interests.

AUTHOR CONTRIBUTIONS

All authors contributed to the study conception and design. Material preparation, data collection, and analysis were performed by David Massa López, Lea Kählau, Katharina Jungnickel, Christian Löw, and Markus Damme. The first draft of the manuscript was written by Markus Damme and all authors commented on previous versions of the manuscript. All authors read and approved the final manuscript.

DATA AVAILABILITY STATEMENT

All data are made available within the manuscript.

REFERENCES

1. Saftig P, Klumperman J. Lysosome biogenesis and lysosomal membrane proteins: trafficking meets function. *Nat Rev Mol Cell Biol*. 2009;10:623-635.
2. Chapel A, Kieffer-Jaquinod S, Sagne C, et al. An extended proteome map of the lysosomal membrane reveals novel potential transporters. *Mol Cell Proteomics*. 2013;12:1572-1588.
3. Abu-Remaileh M, Wyant GA, Kim C, et al. Lysosomal metabolomics reveals V-ATPase- and mTOR-dependent regulation of amino acid efflux from lysosomes. *Science*. 2017;358:807-813.
4. Barriocanal JG, Bonifacino JS, Yuan L, Sandoval IV. Biosynthesis, glycosylation, movement through the Golgi system, and transport to lysosomes by an N-linked carbohydrate-independent mechanism of three lysosomal integral membrane proteins. *J Biol Chem*. 1986;261:16755-16763.
5. Winchester B. Lysosomal metabolism of glycoproteins. *Glycobiology*. 2005;15:1R-15R.
6. Lange PF, Wartosch L, Jentsch TJ, Fuhrmann JC. ClC-7 requires Ostm1 as a beta-subunit to support bone resorption and lysosomal function. *Nature*. 2006;440:220-223.
7. Demirel O, Jan I, Wolters D, et al. The lysosomal polypeptide transporter TAPL is stabilized by interaction with LAMP-1 and LAMP-2. *J Cell Sci*. 2012;125:4230-4240.
8. Yu Z, Surface LE, Park CY, et al. Identification of a transporter complex responsible for the cytosolic entry of nitrogen-containing bisphosphonates. *Elife*. 2018;7:e36620.
9. Massa Lopez D, Thelen M, Stahl F, et al. The lysosomal transporter MFSD1 is essential for liver homeostasis and critically depends on its accessory subunit GLMP. *Elife*. 2019;8:e50025.
10. Fettelschoss V, Burda P, Sagne C, et al. Clinical or ATPase domain mutations in ABCD4 disrupt the interaction between the vitamin B12-trafficking proteins ABCD4 and LMBD1. *J Biol Chem*. 2017;292:11980-11991.
11. Elbein AD, Tropea JE, Mitchell M, Kaushal GP. Kifunensine, a potent inhibitor of the glycoprotein processing mannosidase I. *J Biol Chem*. 1990;265:15599-15605.
12. Pao SS, Paulsen IT, Saier MH Jr. Major facilitator superfamily. *Microbiol Mol Biol Rev*. 1998;62:1-34.
13. Kong XY, Nesset CK, Damme M, et al. Loss of lysosomal membrane protein NCU-G1 in mice results in spontaneous liver fibrosis with accumulation of lipofuscin and iron in Kupffer cells. *Dis Model Mech*. 2014;7:351-362.
14. Gonzalez AC, Schweizer M, Jagdmann S, et al. Unconventional trafficking of mammalian phospholipase D3 to lysosomes. *Cell Rep*. 2018;22:1040-1053.
15. Schieweck O, Damme M, Schroder B, Hasilik A, Schmidt B, Lubke T. NCU-G1 is a highly glycosylated integral membrane protein of the lysosome. *Biochem J*. 2009;422:83-90.
16. Carlsson SR, Fukuda M. Structure of human lysosomal membrane glycoprotein 1. Assignment of disulfide bonds and visualization of its domain arrangement. *J Biol Chem*. 1989;264:20526-20531.
17. Carlsson SR, Fukuda M. The polylactosaminoglycans of human lysosomal membrane glycoproteins lamp-1 and lamp-2. Localization on the peptide backbones. *J Biol Chem*. 1990;265:20488-20495.
18. Kundra R, Kornfeld S. Asparagine-linked oligosaccharides protect Lamp-1 and Lamp-2 from intracellular proteolysis. *J Biol Chem*. 1999;274:31039-31046.
19. Schwappach B, Zerangue N, Jan YN, Jan LY. Molecular basis for K(ATP) assembly: transmembrane interactions mediate association of a K+ channel with an ABC transporter. *Neuron*. 2000;26:155-167.
20. Alguel Y, Cameron AD, Diallinas G, Byrne B. Transporter oligomerization: form and function. *Biochem Soc Trans*. 2016;44:1737-1744.
21. Visser WE, Philp NJ, van Dijk TB, et al. Evidence for a homodimeric structure of human monocarboxylate transporter 8. *Endocrinology*. 2009;150:5163-5170.
22. Leisle L, Ludwig CF, Wagner FA, Jentsch TJ, Stauber T. ClC-7 is a slowly voltage-gated 2Cl(-)/1H(+)-exchanger and requires Ostm1 for transport activity. *Embo J*. 2011;30:2140-2152.
23. Bonifacino JS, Traub LM. Signals for sorting of transmembrane proteins to endosomes and lysosomes. *Annu Rev Biochem*. 2003;72:395-447.
24. Fontenot EB, Ditusa SF, Kato N, et al. Increased phosphate transport of Arabidopsis thaliana Pht1;1 by site-directed mutagenesis of tyrosine 312 may be attributed to the disruption of homomeric interactions. *Plant Cell Environ*. 2015;38:2012-2022.
25. Liu KH, Tsay YF. Switching between the two action modes of the dual-affinity nitrate transporter CHL1 by phosphorylation. *Embo J*. 2003;22:1005-1013.
26. Weinert S, Jabs S, Hohensee S, Chan WL, Kornak U, Jentsch TJ. Transport activity and presence of ClC-7/Ostm1 complex account for different cellular functions. *EMBO Rep*. 2014;15:784-791.

SUPPORTING INFORMATION

Additional supporting information may be found online in the Supporting Information section.

How to cite this article: Massa López D, Kählau L, Esther Julia Jungnickel K, Löw C, Damme M. Characterization of the complex of the lysosomal membrane transporter MFSD1 and its accessory subunit GLMP. *The FASEB Journal*. 2020;34:14695–14709. https://doi.org/10.1096/fj.202000912RR